

Water-Tunnel Studies of Leading-Edge Vortices

Gary E. Erickson*

Northrop Corporation, Hawthorne, Calif.

Flow visualization studies have been made at Northrop in a hydrodynamic facility of leading-edge vortex flows. Vortex core trajectory and stability characteristics have been obtained on wing planforms suitable for subsonic-transonic and supersonic cruise fighter designs. The applicability of results obtained at low Reynolds number in water to higher Reynolds number vortex flow phenomena in air is addressed. Comparisons of water-tunnel vortex positions and burst locations are made with flow visualization results obtained in air. Where appropriate, correlation of water-tunnel vortex flow behavior is made with trends observed in subsonic wind-tunnel data.

Nomenclature

c_0	= wing centerline chord, m
$C_{l\beta}$	= lateral stability parameter ($\partial C_l / \partial \beta$) per degree
L	= longitudinal distance along wing centerline chord measured from apex, m
q_n	= nondimensional normal perturbation velocity
Re	= Reynolds number (based on wing centerline chord, except where otherwise indicated), $V_\infty c_0 / \nu$
TE	= trailing edge
V_∞	= freestream velocity, m/s
x	= vortex breakdown position measured along centerline chord from wing trailing edge, m
Δp	= nondimensional pressure differential across vortex sheet
$\Delta(x/c_0)$	= difference in nondimensional vortex breakdown positions in sideslip
α	= angle of attack, deg
α_{BD-TE}	= angle of attack for vortex breakdown at wing trailing edge, deg
α_{core}	= vortex core angle of attack, deg
β	= sideslip angle, deg
Λ_{LE}	= leading-edge sweep angle, deg
Λ_{core}	= vortex core sweep angle, deg
ϕ	= nondimensional perturbation velocity potential
δ_n	= leading-edge flap deflection angle measured normal to flap hingeline, deg

Introduction

THE flow past thin, slender wings and highly sweptback leading-edge extensions (LEX) or wing-body strakes at moderate-to-high angles of attack is characterized by a leading-edge separation which forms a stable vortex over the lifting surface. This flow situation is illustrated in the Northrop water-tunnel photograph in Fig. 1.

Experimental studies and flight tests on a variety of aircraft have shown that significant increases in maximum lift and reductions in drag at high lift can be obtained by careful generation and control of concentrated vortices which favorably interact with the flow over a moderate-aspect-ratio

main wing surface. These vortex-flow-related improvements lead to an increase in maneuvering performance without large cruise performance penalties. For example, vortex flows developed on wing-LEX geometries have been successfully applied to the Northrop F-5E/F/G and YF-17, Air Force/General Dynamics F-16, and Navy/McDonnell-Douglas/Northrop F/A-18 fighter configurations.

The presence of powerful vortex flows on advanced fighter aircraft influences the lateral-directional as well as longitudinal aerodynamic characteristics. Consequently, an understanding of the fluid mechanics of leading-edge vortex flows and key parameters affecting vortex core trajectory and stability on a variety of wing planforms is desirable to the aerodynamicist/aircraft designer. In addition, knowledge a priori of vortex core trajectories and vortex burst positions would augment the development and implementation of theoretical methods to predict the surface loading characteristics of wings with vortex flows including the effects of vortex breakdown.

The Reynolds number insensitivity of vortex flow characteristics of thin, flat-plate, sharp-edged wings makes

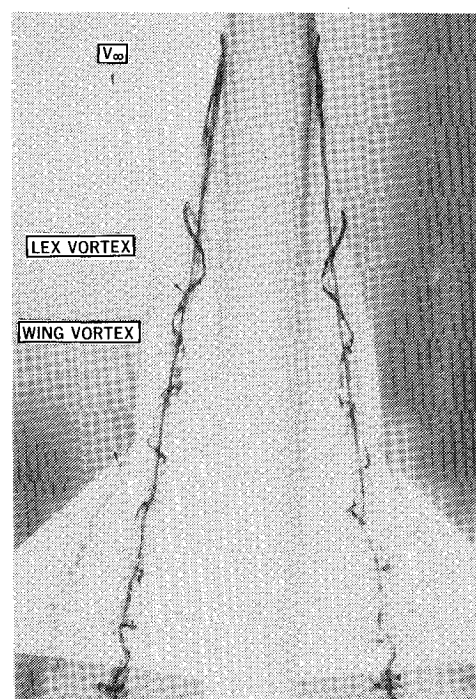


Fig. 1 Water-tunnel flow visualization (by dye injection) of leading-edge vortex flows ($\alpha = 15$ deg).

Presented as Paper 80-1423 at the 13th Fluid and Plasma Dynamics Conference, Snowmass, Colo., July 14-16, 1980; submitted Dec. 22, 1980; revision received Aug. 27, 1981. Copyright © American Institute of Aeronautics and Astronautics, Inc., 1981. All rights reserved.

*Senior Engineer, Aerodynamics Research Department. Member AIAA.

FACILITY	REYNOLDS NO. (BASED ON CENTER- LINE CHORD)
○ NORTHROP	WATER TUNNEL 3.0×10^4
● THOMPSON	WATER TUNNEL 9.8×10^3
+ ERICKSON	WATER TUNNEL 1.0×10^4
□ POISSON-QUINTON	WIND TUNNEL 1.5×10^6
△ POISSON-QUINTON	WIND TUNNEL 1.3×10^6
● WENTZ & KOHLMAN	WIND TUNNEL 9.0×10^5
× HUMMEL & SRINIVASAN	WIND TUNNEL $1.4 \text{ \& } 1.7 \times 10^6$
△ HUMMEL	WIND TUNNEL 2.0×10^6
◇ POISSON-QUINTON	FLIGHT 40.0×10^6
◆ LAMBOURNE & BRYER	WATER TUNNEL $1.0 \text{ \& } 8.0 \times 10^4$
* CHIGIER	WIND TUNNEL 2.0×10^6
▲ EARNSHAW & LAWFORD	WIND TUNNEL 1.0×10^6
◆ POISSON-QUINTON	WATER TUNNEL 3.0×10^4
▨ LOWSON	WATER TUNNEL 3.0×10^4

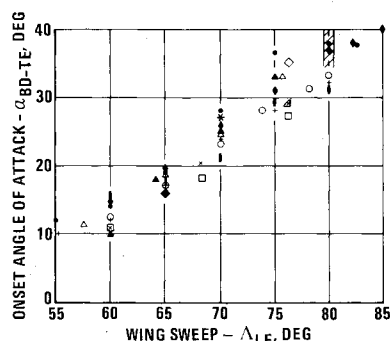
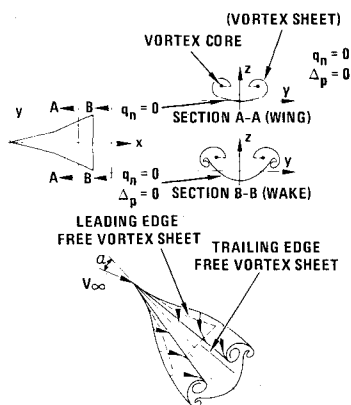


Fig. 2 Effects of delta wing sweep, Reynolds number, and test facility on vortex breakdown onset angle (Ref. 1).

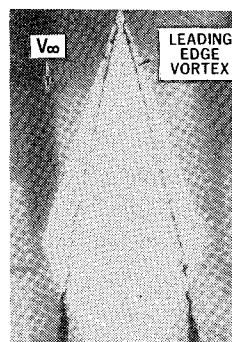
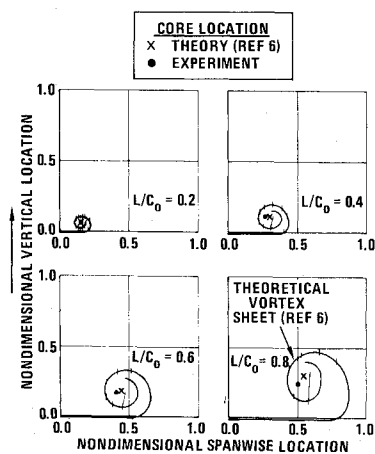
Fig. 3 Schematic of slender wing leading-edge vortex flow.



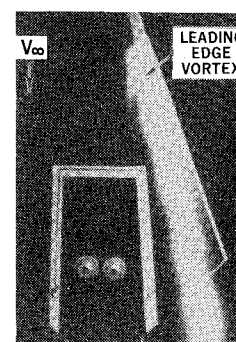
such flow phenomena amenable to investigation in a hydrodynamic facility where the vortices can be visualized at very slow speed and in great detail. The delta wing vortex breakdown characteristics presented in Fig. 2 (from Ref. 1) indicate that the variation in the data due to changes in Reynolds number is no greater than the variation associated with different test facilities, model support arrangements, and methods of flow visualization at the same Reynolds number. The applicability of results obtained in water at low Reynolds numbers to vortex flows at high Reynolds numbers in air has been documented in Refs. 2-5.

The current investigation conducted in the Northrop 0.41×0.61 -meter vertical test section Diagnostic Water Tunnel is intended to provide a data base on leading-edge vortex core trajectory and vortex core stability characteristics. Tests were conducted at a freestream speed of 0.1 m/s corresponding to a Reynolds number of $1 \times 10^5/\text{m}$. (Models tested in the Northrop water tunnel have, typically, a centerline chord of 0.3 m . A description of the water-tunnel facility and test technique is provided in Ref. 5.) Comparisons are made with available flow visualization results in air and, where appropriate, correlations are made with trends observed in subsonic wind-tunnel data.

Fig. 4 Theoretical and experimental vortex core positions on an aspect ratio 1.0 delta wing at $\alpha = 20.5 \text{ deg}$.



NORTHROP WATER TUNNEL - DYE INJECTION



NORTHROP WIND TUNNEL - SMOKE INJECTION

Fig. 5 Water-tunnel and wind-tunnel vortex flow visualization on diamond planforms at $\alpha = 20 \text{ deg}$.

Discussion of Results

Water-Tunnel Vortex Flow Simulation

The flow phenomena which must be simulated in the water tunnel in order to insure correlation are vortex generation, vortex core location, and vortex core breakdown. For thin, sharp-edged wings the boundary layer on the lower surface cannot negotiate the very large pressure gradients at the leading edge and, consequently, a fixed line of separation exists. A sheet of distributed vorticity is shed which, for a highly swept wing, rolls up into a leading-edge spiral vortex with concentrated core (see Fig. 3). Since flow separation occurs at a sharp leading edge whether the lower surface boundary layer is laminar or turbulent, vortex generation is accurately represented in the water tunnel.

A water tunnel is generally operated at Reynolds numbers well below those of wind tunnels and flight. For example, Reynolds numbers are typically of order 10^3 - 10^4 , 10^5 - 10^6 , and 10^7 - 10^8 in water tunnels, wind tunnels, and flight, respectively. For the test results of the water tunnel to truly represent the real situation, the fluid motion under consideration must be of the kind which is insensitive to changes in Reynolds number within the above ranges.

Leading-edge vortex flows can, in general, be divided into three regions: 1) the inviscid flow outside the surface boundary layer, vortex sheet (free shear layer), and vortex core; 2) the boundary-layer flow near the wing; and 3) the vorticity inside the vortex sheet and vortex core. Each regime has its own characteristics.

Consider first the inviscid flow. The flow is governed by the potential flow equation (Laplace equation)

$$\nabla^2 \phi = 0 \quad (1)$$

subject to the boundary conditions (see Fig. 3)

$$q_n = 0 \text{ at the outer edge of the wing boundary layer}$$

and

$$q_n = 0 \quad \Delta p = 0 \text{ on the vortex sheet}$$

In the above, ϕ is the perturbation potential, q_n the normal velocity, and Δp the pressure differential across the sheet. From this set of equations alone, excluding the viscous regions 2 and 3 from consideration, it is possible to determine the location of the vortex sheet and vortex core and, hence, the lift characteristics of the wing. Since the vortex sheet originates from the sharp leading edge, its strength is essentially independent of Reynolds number. Consequently one expects the water tunnel to be capable of simulating the position of the vortex sheet and vortex core, as well as the lift, should the water tunnel have a force measurement capability.

Theoretical and experimental results support this reasoning. Northrop water-tunnel measurements of the location of the vortex core on an aspect ratio 1.0 delta wing at 20.5 deg angle of attack are in reasonable agreement with results from a Northrop nonlinear lifting surface theory⁶ as shown in Fig. 4. The fact that theoretical methods which ignore viscous effects can reasonably predict vortex flow aerodynamics is one indication of the Reynolds number insensitivity of such phenomena. The vortex core path on a 70 deg swept diamond planform at 20 deg angle of attack as observed in the Northrop water tunnel agrees reasonably well with wind-tunnel smoke flow visualization on a similar diamond planform at a Reynolds number of approximately 5×10^5 (based on mean aerodynamic chord) in the Northrop 7 x 10 ft low-speed facility, as shown in Fig. 5.

The second region, the boundary-layer flow, is viscosity dominated. The upper surface boundary-layer flow is separated near the leading edge, generating a secondary vortex having a sense of rotation which is opposite to that of the primary vortex. The secondary separation line and strength and location of the secondary vortex vary with the Reynolds number. Therefore, in water-tunnel tests, the secondary vortex can at most be observed in a qualitative sense.

The third region deals with the internal structure of the vortex flow itself. Vortex cores are regions of concentrated vorticity that can be considered roughly axisymmetric and of continuously distributed vorticity. Within the core are appreciable axial and circumferential, or swirl, velocity components which are strongly coupled. An important physical feature to note concerning a vortex core is its high responsiveness to external disturbances, such that small perturbations outside the core can trigger large responses within the core itself.

The question arises, then, under what flow conditions does the water tunnel provide a realistic representation of the vortex *breakdown* phenomena experienced in wind-tunnel and flight tests? (Vortex breakdown, or bursting, is defined as an abrupt expansion of the vortex flow characterized by a sudden deceleration and stagnation of the core axial flow.) The best correlations of burst position on thin, flat, sharp-edged wings have been at *high angles of attack* where breakdown occurs ahead of the wing trailing edge. These correlations suggest that under certain restrictive conditions the relative importance of inertia, viscous, and pressure terms is simulated in the water tunnel. Water-tunnel experience suggests that the pressure gradient in the external potential flowfield is the dominant parameter at high angles of attack where the flowfield is vortex dominated, that is, the size of the vortex greatly exceeds the undisturbed wing boundary-layer thickness. Provided flow separation occurs simultaneously everywhere along a sharp leading edge, the water tunnel is expected to provide an acceptable representation of the size

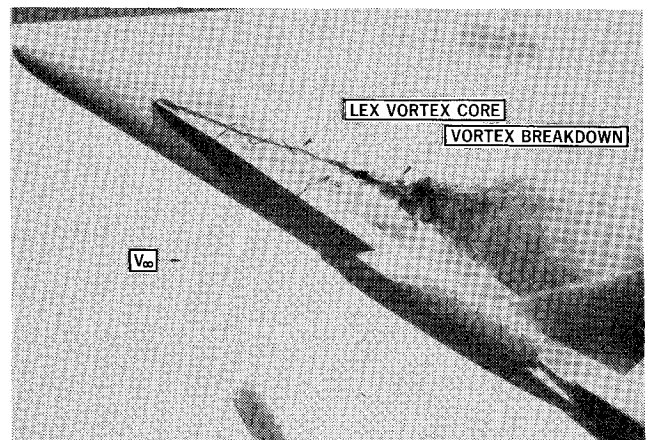


Fig. 6 Vortex-dominated flow on an advanced fighter model at high angle of attack ($\alpha > 30$ deg).

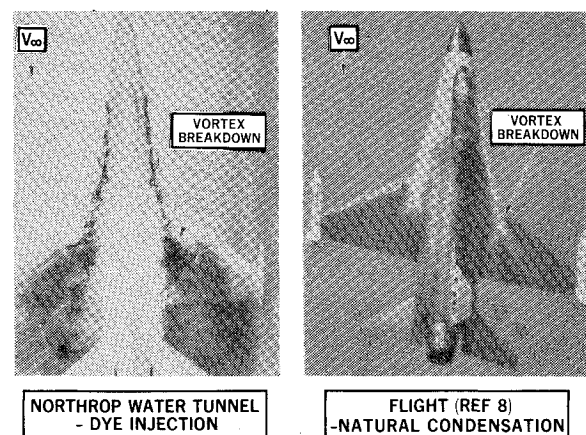


Fig. 7 Qualitative water-to-air correlation of LEX vortex breakdown ($\alpha > 20$ deg).

and structure of the wake shed by a thin, flat-plate wing at high attitude and, hence, the adverse pressure gradient through which the vortex core must traverse. The water-tunnel photograph in Fig. 6 illustrates a vortex-dominated flow situation developed on a small-scale model of an advanced fighter featuring a sharp, highly swept wing leading-edge extension (LEX). Comparison of water-tunnel results with observations of vortex cores (made possible by smoke injection or natural condensation) in Northrop wind-tunnel studies of LEX-wing fighter configurations⁷ indicate that the water-to-air analogy is valid under these conditions.

A water tunnel-to-flight correlation of a *qualitative* nature is shown in Fig. 7 which depicts LEX vortex breakdown on a current fighter aircraft at high angle of attack (angle of attack in each case is similar but wing flap deflections differ). The water-tunnel model (an inexpensive, plastic model) exhibits LEX vortex bursting over the wing panel at a location approximating the burst position on the full-scale aircraft (flight photograph is from Ref. 8). It is upon this premise—the dominance of the adverse pressure gradient—that water-tunnel vortex breakdown results are applied to higher Reynolds number phenomena in air at *high angles of attack*.

Special note should be made of surface flows that are not yet vortex dominated and, consequently, subject to large viscous effects, as would occur at low angles of attack where vortex core/boundary-layer interaction can be significant. Large Reynolds number effects are also evident on wings with round leading edges, deflected flaps, thick sections, etc., where leading-edge flow separation is delayed and a salient edge of separation does not exist. When the vortex burst position is aft of the wing trailing edge (wing pressure field is

Fig. 8 Effect of delta wing leading-edge sweep angle on vortex core sweep angle ($\alpha > 10$ deg).

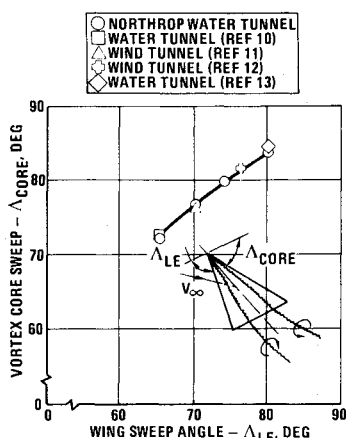
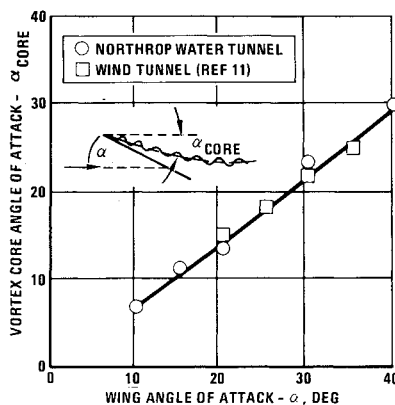


Fig. 9 Effect of 70 deg delta wing angle of attack on vortex core angle of attack.



insufficient to promote vortex breakdown), water-to-air correlations often prove prohibitive due to different model support effects on the downstream pressure gradient and, consequently, vortex stability. Variation of hydrostatic pressure has negligible influence on vortex stability. Rather, it is the pressure changes associated with the fluid motion that affect the burst characteristics of the vortex core. A detailed account of water-to-air correlations of wing and body vortex flow behavior is provided in a recent study funded by the U.S. Air Force/Wright Aeronautical Laboratory.⁹

Wing Sweep and Angle of Attack Effects on Vortex Core Trajectory

Figure 8 presents the effect of delta wing leading-edge sweep angle on vortex core sweep angle, the latter being measured over the linear region of the core prior to streamwise deflection near the wing trailing edge. (Note: The wings tested were flat-plate, aluminum stock, with thickness-to-centerline chord ratios less than 0.01 and sharp, beveled leading edges.) An essentially linear relationship exists between wing sweep and core sweep angles. As far as can be determined in the water tunnel, for the angles of attack considered in the present studies (greater than 10 deg), vortex core sweep for a given wing sweep is relatively insensitive to angle-of-attack changes. The difference between vortex core and wing sweep angles diminishes as wing sweep is increased. Also shown in Fig. 8 are experimental results in water and air from Refs. 10-13 obtained at Reynolds numbers of 10^4 - 10^6 which are consistent with the present results.

Variation of vortex core angle of attack with wing angle of attack is presented in Fig. 9 for a 70 deg delta wing. A linear relationship exists between wing and vortex core angles of attack, the latter being measured over the region where vortex core height above the wing varies linearly with distance downstream. For comparison, wind-tunnel measurements of vortex core position using a laser anemometer at a Reynolds number of about 10^6 obtained in Ref. 11 are also shown in Fig. 9.

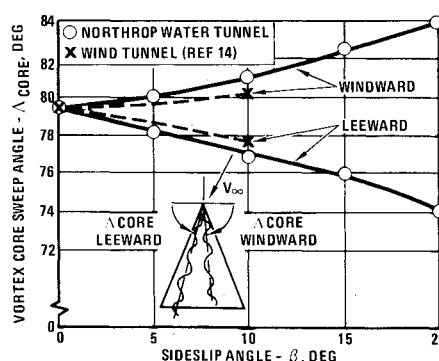


Fig. 10 Effect of sideslip on 74 deg delta wing vortex core sweep angles ($\alpha = 20$ deg).

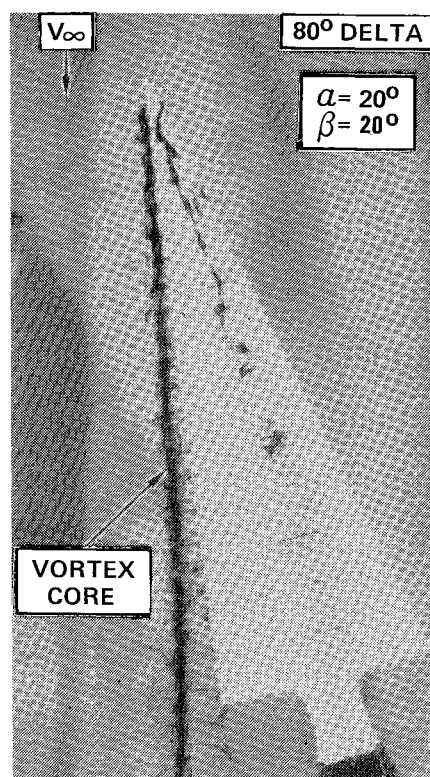


Fig. 11 Water-tunnel photograph of leeward vortex path at large sideslip.

Sideslip Effects on Vortex Core Trajectory

The effect of sideslip on 74 deg delta wing windward and leeward vortex core sweep angles is presented in Fig. 10. The water-tunnel data indicate that a 5 deg increase in sideslip results in approximately a 1 deg increase and decrease in windward and leeward vortex core sweep angles, respectively. Wind-tunnel results obtained at a Reynolds number of approximately 3×10^5 (based on mean aerodynamic chord) in Ref. 14 using water vapor are also shown in Fig. 10, revealing similar trends with sideslip.

In a sideslip condition, the leeward vortex core is displaced outboard and upward over the wing relative to the windward vortex core. This results in an asymmetry in angles between the vortex cores and wing surface and wing symmetry plane.

It is interesting to note that at sideslip angles at which the leeward wing leading edge is swept 90 deg or greater (that is, the leading edge is now a "trailing edge"), a discrete vortex is still in evidence. This flow situation is illustrated in Fig. 11 and is consistent with theoretical flow streamlines presented in Ref. 15. A similar vortex motion is observed at the trailing edge of a forward swept wing.⁹

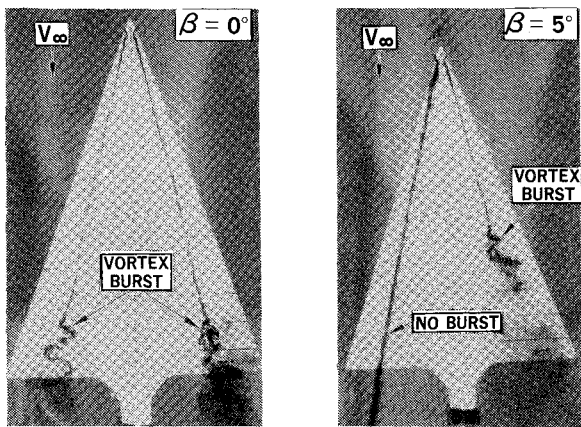


Fig. 12 Effect of sideslip on 70 deg delta wing vortex core stability ($\alpha = 25$ deg).

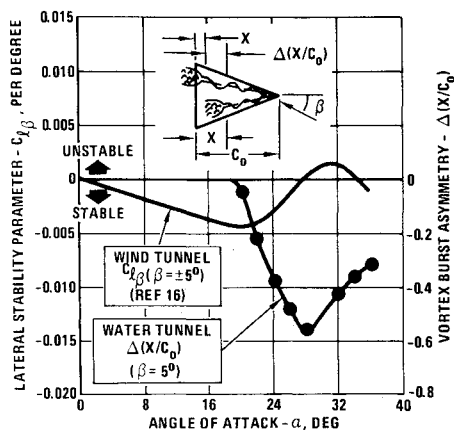


Fig. 13 Comparison of water-tunnel vortex burst asymmetry and wind-tunnel lateral stability characteristics (70 deg delta wing).

Sideslip Effects on Vortex Core Stability

Results depicting the effect of sideslip on leading-edge vortex stability are presented in Fig. 12 for a 70 deg delta wing. (The water-tunnel data are uncorrected for tunnel wall effects.) Results reveal vortex burst position asymmetry due to sideslip. The degree of asymmetry at a given angle of attack increases with increased sideslip angle.

Vortex burst asymmetry $\Delta(x/c_0)$ is defined as the difference in burst location over the wing between windward and leeward sides. Burst location x is measured from the wing trailing edge and is normalized by the wing centerline chord c_0 . This parameter correlates with lateral stability trends determined in wind-tunnel tests of delta wings in Ref. 16 at a Reynolds number of approximately 10^6 , as illustrated in Fig. 13. Initial reduction in the slope of the curve showing the lateral stability parameter $C_{l\beta}$ vs angle of attack corresponds reasonably well with initial vortex breakdown asymmetry. Maximum reduction in lateral stability level occurs at approximately the angle of attack at which vortex breakdown asymmetry is maximum. Burst position asymmetry is reduced with further increase in angle of attack and correspondingly favorable increments in $C_{l\beta}$ are observed.

Deflected Flap Effects on Vortex Stability

Downward deflection of a plain trailing-edge flap results in an increase in the positive (adverse) pressure gradient near the wing trailing edge and, hence, a reduction in vortex stability as discussed in Ref. 17. The maximum vortex-induced lift increment is reduced since the vortices burst at a lower angle of attack. Increased trailing-edge flap deflection angle results in a further reduction in vortex stability at a given angle of attack. This flap effect is evident throughout the high angle-

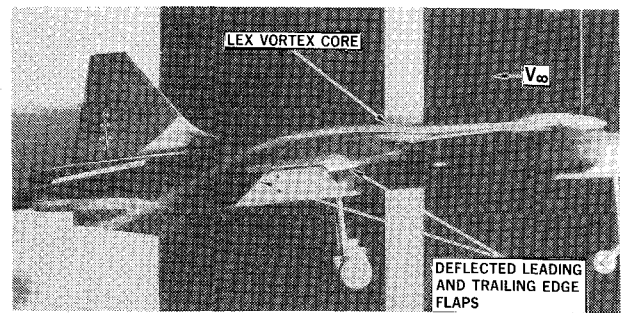


Fig. 14 Wind-tunnel smoke flow visualization of a LEX vortex core at $\alpha = 6$ deg ($Re = 5 \times 10^5$ based on mean aerodynamic chord).

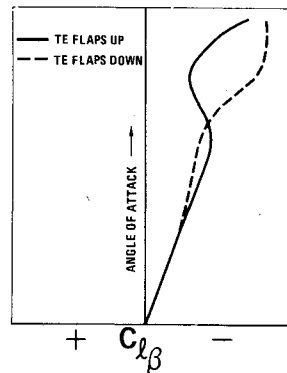


Fig. 15 Effect of deflected trailing-edge flaps on lateral stability of a twin-jet fighter ($Re = 1.5 \times 10^6$ based on mean aerodynamic chord).

of-attack range, which is indicative of the effective increase in angle of attack due to positive aft camber.

The vortex core trajectory is also affected by the deflected flap such that at angles of attack prior to bursting, the core tends to follow the curvature of the wing, as shown in the Northrop wind-tunnel smoke flow visualization photograph¹⁸ in Fig. 14. This, in turn, may result in vortex flow interaction with an aft-mounted horizontal tail surface, hence affecting longitudinal stability. This phenomenon may not be evident in a water tunnel, however, due to laminar boundary-layer separation on the wing. Entrainment of turbulent fluid from the separated boundary layer into the vortex core can promote premature bursting of the vortex.⁹

By similar reasoning, the adverse effect of trailing-edge flap deflection on vortex stability is underpredicted at low Reynolds numbers in a water tunnel. It has been observed on a LEX-wing fighter configuration^{9,18} that the water tunnel reveals the correct trends associated with deflected plain trailing-edge flaps. The adverse effects on vortex stability in water, however, are considerably less than the corresponding effects observed in air at higher Reynolds number.

It is not intended to leave the impression that a trailing-edge flap deflection is undesirable. A deflected trailing-edge flap increases the potential flow lift so that for a constant lift coefficient less vortex lift is needed, less angle of attack is required, and the drag is likely to be lower.

In sideslip conditions, water-tunnel observations indicate that a deflected plain trailing-edge flap tends to reduce the vortex burst asymmetry exhibited with flaps retracted. The leeward vortex strength is reduced somewhat relative to the windward vortex (based on water-tunnel observation of a tighter coiling of the windward vortex) and, consequently, cannot as easily traverse the positive pressure gradient associated with the deflected flap. Examination of low-speed wind-tunnel data¹⁷ on a twin-jet fighter configuration reveals an increase in lateral stability at high angles of attack due to deflected plain trailing-edge flaps as illustrated in Fig. 15. Since the primary contributor to static lateral stability is the wing, the increase in lateral stability may be associated with a reduction in vortex burst asymmetry.

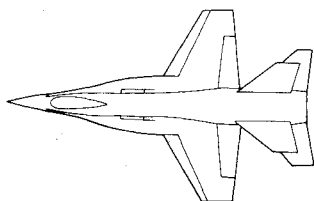


Fig. 16 Leading-edge flap effects on LEX vortex breakdown at the trailing edge (water tunnel, dye injection; wind tunnel, smoke injection).

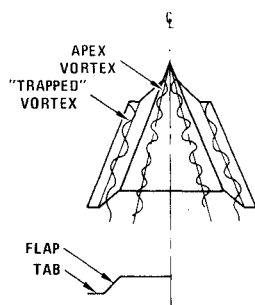
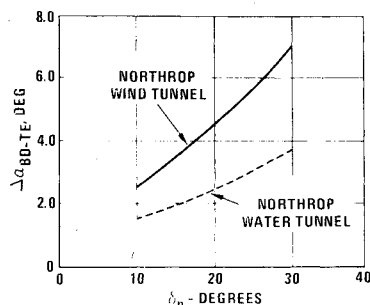
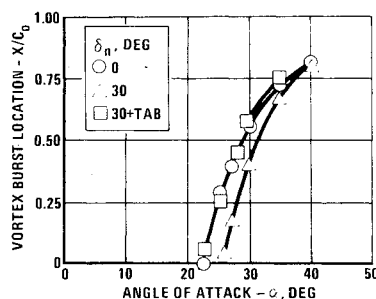


Fig. 17 "Vortex flap" effect on 74 deg delta wing apex vortex stability.



Deflection of a leading-edge flap has a stabilizing influence on the leading-edge vortex, since it reduces the pressure peak and the associated positive pressure gradient near the wing nose. This effect is illustrated in Fig. 16 for a LEX-wing configuration. A 30 deg flap deflection angle, for example, results in a significant increase in angle of attack for vortex bursting at the trailing edge of the wing. The water-tunnel results, when compared with low-speed wind-tunnel data obtained on a similar configuration at a Reynolds number of 5×10^5 (based on mean aerodynamic chord) from Ref. 18, show a less beneficial effect on vortex stability due to leading-edge flap deflection (see Fig. 16). This disparity can also be attributed to the laminar boundary-layer separation characteristics at low Reynolds number in the water tunnel which tend to promote vortex core instability.

A deflected leading-edge flap reduces the vortex-induced lift, that is, the vortex strength is reduced at a given angle of attack. This effect can be viewed in a qualitative manner in the water tunnel by observing the less tightly wound vortex flow with flaps down. At higher angles of attack at which flow separation occurs at the flap leading edge, the subsequent formation of a primary leading-edge vortex on the deflected flap may result in induced-drag benefits due to the

vortex suction pressures acting on the forward-facing surface.¹⁹

"Vortex Flap" Effects on Vortex Trajectory and Stability

A promising means of improving the drag characteristics at cruise and maneuver conditions is to "force" the flow to separate in a controlled manner at the leading edge, roll up into a discrete vortex core, and confine the vortex to a region near the leading edge by suitable contouring of the wing profiles. Drag benefits are thus made possible by allowing the vortex to run along a sloping surface which has a forward-facing component in streamwise projection. Such concepts have received attention at Northrop during the development of the YF-17 leading-edge extension¹⁸ and in water-tunnel studies (unpublished data) of slender wings suitable for supercruise fighters, at NASA Langley Research Center on supercruise configurations,¹⁹ and at the Boeing Company on commercial SST and supercruise fighter configurations.²⁰

For the 74 deg delta wing shown in Fig. 17, a leading-edge tab was added to the deflected flap such that the tab deflection was zero relative to the wing plane. The resultant leading-edge flap arrangement is similar to the "vortex flap" concept discussed in Ref. 20. The data shown in Fig. 17 indicate that the primary apex vortex stability increase associated with the deflected leading-edge flap is lost when the tab is present. Water-tunnel observations reveal the presence of a primary vortex flow at low angles of attack within the confines of the flap arrangement in addition to the primary vortex pair shed from the apex. The "trapped vortex" tends to remain within this leading-edge channel for a limited distance downstream but, as the vortex grows in size, the core trajectory abruptly turns streamwise, "escaping" the channel. Previous studies in the Northrop water tunnel (unpublished data) have indicated that vortex core path can be altered by leading-edge contouring at the expense of vortex stability. It should also be noted that attainment of drag benefits by forcing the vortex to act on a sloping surface are, in general, concurrent with a reduction in vortex-induced lift.

Summary

Northrop has conducted flow visualization studies in a hydrodynamic test facility of leading-edge vortex flow characteristics. Vortex core trajectory and core stability characteristics have been obtained on a variety of wing planforms having sweep angles ranging from approximately 60-80 deg. The water tunnel has been shown to provide a reasonable estimate of thin, flat-plate, sharp-edged wing leading-edge vortex core positions to be expected at higher Reynolds numbers in air. At high angles of attack where potential flow effects dominate, vortex breakdown locations in water are seen to be in reasonable agreement with wind-tunnel and flight test results. In most cases, however, viscous effects on vortex behavior preclude quantitative water-to-air comparisons. A water tunnel has shown utility, however, in assessing in a qualitative manner the effects of deflected leading- and trailing-edge flaps and leading-edge contouring on the vortex characteristics of simple wing planforms and scale models of complete fighter configurations.

References

- 1 Erickson, G.E., "Flow Studies of Slender Wing Vortices," Paper 80-1423 presented at the 13th AIAA Fluid and Plasma Dynamics Conference, Snowmass, Colo., July 14-16, 1980.
- 2 Poisson-Quinton, P. and Werle, H., "Water Tunnel Visualization of Vortex Flow," *Astronautics and Aeronautics*, June 1967.
- 3 Werle, H., "Structures Des Decollements Sur Les Ailes en Fleche," *La Recherche Aerospatiale*, 1980-2, pp. 85-108.
- 4 Erickson, G.E., "Water Tunnel Flow Visualization: Insight Into Complex Three-Dimensional Flow Fields," AIAA Paper 79-1530, July 1979.
- 5 Lorincz, D.J., "Water Tunnel Flow Visualization Study of the F-15," NASA CR-144878, 1978.

⁶Shen, C., "Northrop Nonlinear Lifting Surface Theory," unpublished data, 1977.

⁷Headley, J.W., "Analysis of Wind Tunnel Data Pertaining to High Angle of Attack Aerodynamics," Vol. I, AFFDL-TR-78-14, 1978.

⁸*Aviation Week and Space Technology*, Vol. III, No. 1, July 2, 1979, pp. 20-21.

⁹Erickson, G.E., "Vortex Flow Correlation," AFWAL-TR-80-3143, Jan. 1981.

¹⁰Lambourne, N.C. and Bryer, D.W., "The Bursting of Leading-Edge Vortices—Some Observations and Discussion of the Phenomenon," R.&M. No. 3282, ARC, Vol. 22, April 1961, p. 775.

¹¹Chigier, N.A., "Measurement of Vortex Breakdown Over a Delta Wing Using a Laser Anemometer," NEAR TR 62, June 1974.

¹²Hummel, D., "Experimental Investigation of the Flow on the Suction Side of a Thin Delta Wing," *Z. Flugwiss.*, Vol. 13, July 1965, pp. 247-252.

¹³Lowson, M.V., "Some Experiments with Vortex Breakdown," *Journal of Royal Aeronautical Society*, Vol. 68, 1964, p. 343.

¹⁴Wentz, W.H., "Effects of Leading-Edge Camber on Low-Speed Characteristics of Slender Delta Wings," NASA CR-2002, Oct. 1972.

¹⁵Küchemann, D., *The Aerodynamic Design of Aircraft*, Pergamon Press, New York, 1978, p. 360.

¹⁶Shanks, R.E., "Low-Subsonic Measurements of Static and Dynamic Stability Derivatives of Six Flat-Plate Wings Having Leading-Edge Sweep Angles of 70° to 84°," NASA TN D-1822, 1953.

¹⁷Skow, A.M., Titiriga, A., and Moore, W.A., "Forebody/Wing Vortex Interactions and Their Influence on Departure and Spin Resistance," AGARD-CP-247, Oct. 1978.

¹⁸Gerhardt, H.A., "The Aerodynamic Development of the Wing Root Leading Edge Extension of the P530 Airplane Configuration," Northrop Corp., Aircraft Div., NOR 73-71, 1972.

¹⁹Lamar, J.E., Schemensky, R.T., and Reddy, C.S., "Some Applications of Vortex Flow Analysis Methods Related to the Design of Slender Cambered Wings," AIAA Paper 80-0327, Jan. 1980.

²⁰Tinoco, E.N. and Yoshihara, H., "Subcritical Drag Minimization for Highly Swept Wings with Leading Edge Vortices," AGARD-CP-247, Oct. 1978.

From the AIAA Progress in Astronautics and Aeronautics Series..

AERODYNAMIC HEATING AND THERMAL PROTECTION SYSTEMS—v. 59 HEAT TRANSFER AND THERMAL CONTROL SYSTEMS—v. 60

Edited by Leroy S. Fletcher, University of Virginia

The science and technology of heat transfer constitute an established and well-formed discipline. Although one would expect relatively little change in the heat transfer field in view of its apparent maturity, it so happens that new developments are taking place rapidly in certain branches of heat transfer as a result of the demands of rocket and spacecraft design. The established "textbook" theories of radiation, convection, and conduction simply do not encompass the understanding required to deal with the advanced problems raised by rocket and spacecraft conditions. Moreover, research engineers concerned with such problems have discovered that it is necessary to clarify some fundamental processes in the physics of matter and radiation before acceptable technological solutions can be produced. As a result, these advanced topics in heat transfer have been given a new name in order to characterize both the fundamental science involved and the quantitative nature of the investigation. The name is Thermophysics. Any heat transfer engineer who wishes to be able to cope with advanced problems in heat transfer, in radiation, in convection, or in conduction, whether for spacecraft design or for any other technical purpose, must acquire some knowledge of this new field.

Volume 59 and Volume 60 of the Series offer a coordinated series of original papers representing some of the latest developments in the field. In Volume 59, the topics covered are 1) The Aerothermal Environment, particularly aerodynamic heating combined with radiation exchange and chemical reaction; 2) Plume Radiation, with special reference to the emissions characteristic of the jet components; and 3) Thermal Protection Systems, especially for intense heating conditions. Volume 60 is concerned with: 1) Heat Pipes, a widely used but rather intricate means for internal temperature control; 2) Heat Transfer, especially in complex situations; and 3) Thermal Control Systems, a description of sophisticated systems designed to control the flow of heat within a vehicle so as to maintain a specified temperature environment.

Volume 59—432 pp., 6 × 9, illus. \$20.00 Mem. \$35.00 List

Volume 60—398 pp., 6 × 9, illus. \$20.00 Mem. \$35.00 List

TO ORDER WRITE: Publications Dept., AIAA, 1290 Avenue of the Americas, New York, N.Y. 10019